Polar optical vibrational modes in quantum dots

E. Roca
Department of Theoretical Physics, Havana University, Vedado, 10400 Havana, Cuba

C. Trallero-Giner* and M. Cardona
Max-Planck-Institut für Festkörperforschung, Heisenbergstrasse 1, D-70569 Stuttgart, Federal Republic of Germany
(Received 10 December 1993)

A macroscopic continuum model coupling the mechanical vibrational amplitude and electrostatic potential is applied to obtain the optical vibrational modes in quantum-dot structures. A unified method of solution (valid for any type of nanostructure) that reduces the four coupled second-order differential equations to Helmholtz's and Laplace's equations is described. Analytical solutions for the vibrational amplitude and the Fröhlich-type electron-phonon interaction are given for quantum dots with spherical geometry. The existence of surface modes and their relation to the matching boundary conditions are studied. A qualitative discussion of the ir and Raman activity of the calculated modes is given together with a comparison with the few existing experimental data.

I. INTRODUCTION

The investigation of polar optical vibrations (phonons) in semiconductor nanostructures has been a subject of great interest in the last years. The theoretical treatment of several physical properties, such as electron scattering rates, polaron effects, Raman scattering efficiencies, hot-electron phenomena, etc., requires a reliable description of phonon modes and electron-phonon interaction potentials in such structures. A macroscopic treatment of optical phonons in small spheroidal crystal has been used in the past.[1–3] The so-called Fröhlich frequency[1] and surface modes[2,3] in microcrystals with different geometries were calculated in the framework of dielectric models which neglect the important effect of mechanical boundary conditions.[4]

Today, several advanced technologies permit the growth of semiconductor microcrystals with quasi-zero-dimensional properties (quantum dots). The diameter of these microcrystals is in the range of a few nanometers. Characteristic physical properties appear which suggest a broad spectrum of device applications. Consequently, the energy spectrum and optical properties of quantum dots (QD's) of materials such as CdS,[5] CdSe,[6] GaAs[7], InSb,[8] and Si (Ref. 9) are being extensively studied. Several spectroscopic techniques, including Raman scattering, have been used to investigate confined LO-phonon,[10,11] surface optical phonon,[12,13] and confined acoustic phonon modes.[3,14,15] However, few theoretical treatments of ultrasmall spherical microcrystals have appeared. The Fröhlich polar electron-phonon interaction has been evaluated in Ref. 16. Here the classical dielectric model, neglecting dispersion of the corresponding bulk phonon branches, was used to derive longitudinal-phonon-like modes and the surface optic eigenfunctions. Confined LO phonons, and the corresponding electron-phonon interaction, have been obtained upon application of spherical boundary conditions.[17] However, those models do not take into account the coupling between longitudinal and transverse modes demanded by the matching boundary conditions.[4,18,19] The assumption of a vibrational field of purely longitudinal nature is, in general, unjustified in systems with a surface discontinuity.[4]

In this paper, we develop a long-wavelength macroscopic model for polar optical phonons in QD's. The model takes into account phonon dispersion up to quadratic terms in the wave vector and the coupling between the mechanical vibration displacement, $\vec{u}$ and the electrostatic potential Φ. This treatment requires the solution of a complicated system of four coupled differential equations for $\vec{u}$ and Φ in the quantum dots and the surrounding medium. In what follows we shall describe a method leading to generate analytical solutions of these equations for the case of a material with isotropic dielectric response and vibrational dispersion relations. The general equations and matching boundary conditions for a phenomenological description of long-wavelength polar optical modes in nanostructures with arbitrary shape have been given in Refs. 4, 20, and 21. We consider a single quantum dot of radius R and assume that the constituent materials are isotropic and homogeneous. In such case, we have an equation of motion for the mechanical displacement vector $\vec{u}$ which takes the form

$$\rho(r)\left[\omega^2-\omega_{\rm TO}^2(r)\right]\vec{u}=\vec{\nabla}\left[\rho(r)\beta_L^2(r)\vec{\nabla}\cdot\vec{u}\right]-\vec{\nabla}\times\left[\rho(r)\beta_T^2(r)\vec{\nabla}\times\vec{u}\right]+\alpha(r)\vec{\nabla}\Phi, \quad (1)$$

where $\omega_{\rm TO}$ is the TO bulk phonon frequency, ρ the reduced-mass density, β_L and β_T are phenomenological parameters estimated from the experimental phonon dispersion relations of the corresponding bulk material, and the coefficient α is given by

$$\alpha = \sqrt{\frac{(\varepsilon_0 - \varepsilon_\infty)\rho\omega_{\rm TO}^2}{4\pi}}\ , \tag{2}$$

ε_0 and ε_∞ being the static and high frequency dielectric constants, respectively. In Eq. (1) $\vec{u} = \vec{u}_+ - \vec{u}_-$ is the relative displacement of cation (+) and anion (−) for a given mode. Simultaneously, we must fulfill the equation for the electric field $\vec{E} = -\vec{\nabla}\Phi$

$$\vec{\nabla}\cdot\left(\varepsilon_\infty\vec{\nabla}\Phi\right) = 4\pi\vec{\nabla}\cdot(\alpha\vec{u}). \tag{3}$$

In Eqs. (1) and (3) retardation effects are neglected and a harmonic time dependence $\vec{u}(\vec{r},t) = \vec{u}(\vec{r})e^{-i\omega t}$ is assumed. We note that the scalar potential Φ is a solution of a generalized Poisson equation where $\nabla\cdot(-\alpha\vec{u})$ plays the role of a charge density. Thus, the potential Φ can be thought of as created by the polarization field $\vec{P}$ which is given by[22]

$$\vec{P} = \alpha\vec{u} - \frac{\varepsilon_\infty - 1}{4\pi}\vec{\nabla}\Phi. \tag{4}$$

The matching boundary conditions can be explicitly derived from Eqs. (1) and (3),[4,21] which describe an inhomogeneous system where the material parameters depend on the position coordinate r. An abrupt interface is an extreme case of such inhomogeneities. Equations (1) and (3) are four coupled second-order partial differential equations for $\vec{u}$ and Φ. Thus we must require continuity of the three components of $\vec{u}$ and of Φ at the interface $r = R$ of the spherical quantum dot.

$$\vec{u}|_{r=R_-} = \vec{u}|_{r=R_+}\ , \quad \Phi|_{r=R_-} = \Phi|_{r=R_+}\ . \tag{5}$$

According to Gauss's theorem and for the case of piecewise continuous parameters with only interface discontinuities, from Eqs. (1) and (3) follows the continuity at the interface of the normal component of the mechanical stress tensor $\overleftrightarrow{\sigma}_N$

$$\overleftrightarrow{\sigma}\cdot\vec{N} = -\Big(\rho(\beta_L^2 - 2\beta_T^2)\vec{\nabla}\cdot\vec{u}\,\overleftrightarrow{I} + \rho\beta_T^2\sum_{i,j}(\nabla_i u_j + \nabla_j u_i)\Big)\cdot\vec{N} \tag{6}$$

and the electric displacement[20,21]

$$\vec{D}\cdot\vec{N} = -(-4\pi\alpha\vec{u} + \varepsilon_\infty\vec{\nabla}\Phi)\cdot\vec{N}, \tag{7}$$

where $\vec{N}$ is a unit vector normal to the QD's surface. It is clear that the above matching boundary conditions together with Eqs. (1) and (3) couple longitudinal and transverse fields. Moreover, the modes have a mixed character involving a mechanical vibration $\vec{u}$ and an electrostatic potential.

II. GENERAL SOLUTION

Here, we present a method for solving the above four coupled differential equations. The full solution can be found with the help of an auxiliar scalar function Λ and a vector function $\vec{\Gamma}$, such that

$$\Lambda = \vec{\nabla}\cdot\vec{u} \quad \text{and} \quad \vec{\Gamma} = \vec{\nabla}\times\vec{u}. \tag{8}$$

Applying the curl operator to Eq. (1) and using the vector identity $\vec{\nabla}\times\vec{\nabla}\times\vec{u} = \vec{\nabla}\vec{\nabla}\cdot\vec{u} - \vec{\nabla}^2\vec{u}$, the vector equation

$$(\vec{\nabla}^2 + Q^2)\vec{\Gamma} = 0, \tag{9}$$

follows, where

$$Q^2 = \frac{\omega_{\rm TO}^2 - \omega^2}{\beta_T^2}. \tag{10}$$

Similarly, taking the divergence of Eq. (1) the equation for Λ becomes

$$(\vec{\nabla}^2 + q^2)\Lambda = 0, \tag{11}$$

with

$$q^2 = \frac{\omega_{\rm LO}^2 - \omega^2}{\beta_L^2} \tag{12}$$

and $\omega_{\rm LO}^2 = (\varepsilon_0/\varepsilon_\infty)\omega_{\rm TO}^2$ is the Lydane-Sachs-Teller relation.

After substitution of (8) into (3) the latter is transformed into

$$\vec{\nabla}^2\Phi = \frac{4\pi\alpha}{\varepsilon_\infty}\Lambda, \tag{13}$$

valid for each portion of isotropic and homogeneous material with the appropriate parameters α and ε_∞.

Comparing (11) and (13) we see that the general solution for the scalar potential is given by

$$\Phi = \Phi_H - \frac{4\pi\alpha}{\varepsilon_\infty q^2}\Lambda, \tag{14}$$

where Φ_H is the solution of Laplace's equation

$$\vec{\nabla}^2\Phi_H = 0 \tag{15}$$

and the term proportional to Λ in (14) a particular solution of (13). The vector displacement $\vec{u}$ can be obtained replacing Eqs. (8) and (14) into Eq. (1). After simple manipulation it is straightforward to show that

$$\vec{u} = -\vec{\nabla}\left[\frac{\alpha}{\rho\beta_T^2 Q^2}\Phi_H + \frac{\Lambda}{q^2}\right] + \frac{1}{Q^2}\vec{\nabla}\times\vec{\Gamma}. \tag{16}$$

The above results of Φ and $\vec{u}$ are completely independent of the type of nanostructure (quantum dots, quantum wires, etc.), provided it is composed of isotropic and homogeneous parts separated by interfaces, and of its geometry and matching boundary conditions. For each particular case it is necessary to obtain the general solution of Helmholtz's equation for Λ and $\vec{\Gamma}$ and of Laplace equation for Φ_H within each medium and to match them at the interfaces. For a spherical QD the bounded solutions of Φ_H and Λ are given by

$$\Phi_H = Y_{lm}(\theta,\varphi)\begin{cases} C_1 r^l, & r<R \\ C_2 r^{-l-1}, & r>R, \end{cases} \tag{17}$$

and

$$\Lambda = Y_{lm}(\theta,\varphi)\begin{cases} A_1 j_l(qr), & r<R \\ A_2 h_l^{(1)}(qr), & r>R, \end{cases} \tag{18}$$

where $Y_{lm}(\theta,\varphi)$ with $m=-l,\ldots,l$ and $l=0,1,\ldots$ are the spherical harmonics, j_l and $h_l^{(1)}$ the Bessel and Hankel spherical functions, and C_i, A_i $(i=1,2)$ constants to be determined through the matching procedure. As already emphasized all material parameters entering in (14) and (16) change their value abruptly from one medium to another, i.e., they display steplike dependence on r for $r=R$.

Combining Eqs. (14), (17), and (18) the scalar potential can be written as

$$\Phi(r,\theta,\varphi) = Y_{lm}(\theta,\varphi)\begin{cases} -\dfrac{4\pi\alpha_1}{\varepsilon_\infty^{(1)} q_1^2} A_1 j_l(q_1 r) + C_1 r^l, \\ r<R \\ -\dfrac{4\pi\alpha_2}{\varepsilon_\infty^{(2)} q_2^2} A_2 h_l^{(1)}(q_2 r) + C_2 r^{-l-1}, \\ r>R. \end{cases} \tag{19}$$

The parameters α_i, q_i, and $\varepsilon_\infty^{(i)}$ $(i=1,\ 2)$ take values corresponding to each bulk constituent medium [$i=1$ (2) inside (outside) the sphere]. The solutions for $\vec{\Gamma}$ and $\vec{\nabla}\times\vec{\Gamma}$ are given in the Appendix. Hence, in the curvilinear basis $(\vec{e}_r,\ \vec{X}_{lm},\ \vec{e}_r\times\vec{X}_{lm})$, where X_{lm} is defined by Eq. (A11), the expression for the vector displacement $\vec{u}$ is given by

$$\vec{u} = \left[-\frac{A_1}{q^2}\frac{d}{dr}(j_l) + \frac{B_1 l(l+1)}{rQ^2} g_l - \frac{\alpha C_1}{\rho\beta_T^2 Q^2} l r^{l-1}\right] Y_{lm}\vec{e}_r$$
$$-i\frac{D_1}{Q}\sqrt{l(l+1)}\, g_l \vec{X}_{lm} - i\frac{\sqrt{l(l+1)}}{r}\left[-\frac{\alpha C_1}{\rho\beta_T^2 Q^2} r^l - \frac{A_1}{q^2} j_l + \frac{B_1}{Q^2}\frac{d}{dr}(r g_l)\right]\vec{e}_r\times\vec{X}_{lm}\ ,\quad r<R, \tag{20}$$

where the function g_l is defined in (A7) and B_1, D_1 are additional constants. A similar expression can be written for $r>R$. It is rather useful to express the stress tensor $\overleftrightarrow{\sigma}$ as a function of Λ and $\vec{\Gamma}$. By adding and subtracting $\rho\beta_T^2\nabla_j u_i/2$ to Eq. (6), it is easy to show that

$$\sigma_{ij} = -\rho(\beta_L^2 - 2\beta_T^2)\Lambda - \rho\beta_T^2\left[2\nabla_j u_i + \epsilon_{ijk}\Gamma_k\right], \tag{21}$$

where ϵ_{ijk} is the Levi-Civita tensor and g_{ij} the metric tensor. Einstein's summation convention has been used in (21). The above equation has the same form in all orthogonal curvilinear coordinates. In the particular case of a spherical quantum dot the components of $\overleftrightarrow{\sigma}\cdot\vec{e}_r$ ($\vec{e}_r$ represents the unit vector along $\vec{r}$) refered to the curvilinear basis $(\vec{e}_r,\ \vec{X}_{lm}/|\vec{X}_{lm}|,\ \vec{e}_r\times\vec{X}_{lm}/|\vec{X}_{lm}|)$, where $\vec{X}_{lm}$ is defined in Eq. (A11), become

$$\sigma_{1r} = -2\beta_T^2\rho\left[\left(\frac{\beta_L^2-2\beta_T^2}{2\beta_T^2} j_l - \frac{1}{q^2}\frac{d^2}{dr^2}(j_l)\right) A_1 + l(l+1)\frac{B_1}{Q^2}\frac{d}{dr}\left(\frac{g_l}{r}\right) - \frac{\alpha C_1}{\rho\beta_T^2 Q^2} l(l-1) r^{l-2}\right]\cdot Y_{l,m}(\theta,\varphi)\ , \tag{22}$$

$$\sigma_{2r} = +\frac{i\rho\beta_T^2}{Q} D_1\sqrt{l(l+1)}\, r\frac{d}{dr}\left(\frac{g_l}{r}\right)|\vec{X}_{lm}|\ , \tag{23}$$

$$\sigma_{3r} = +i2\rho\beta_T^2\sqrt{l(l+1)}\left\{-\frac{\alpha C_1}{\rho\beta_T^2 Q^2}(l-1) r^{l-2} - \frac{A_1}{q^2}\frac{d}{dr}\left(\frac{j_l}{r}\right) + \frac{B_1}{Q^2}\left[g_l - 2\frac{d}{dr}\left(\frac{1}{r}\frac{d}{dr}(r g_l)\right)\right]\right\}|\vec{X}_{lm}|, \tag{24}$$

where the indices (1 or 2, 3) represent the components along $\vec{e}_r$, $\vec{X}_{lm}$, and $\vec{e}_r\times\vec{X}_{lm}$, respectively.

III. COMPLETE SET OF CONFINED MODES

We consider next a quantum dot of GaAs in an AlAs matrix where approximate, more restrictive matching boundary conditions can be applied.[23] Here, the continuity of Φ at the interface must still be imposed but the conditions (5) – (7) can be approximately reduced to

$$\vec{u}|_{r=R} = 0, \tag{25}$$

$$\varepsilon_\infty^{(1)}\left.\frac{\partial\Phi}{\partial r}\right|_{r=R_-} = \varepsilon_\infty^{(2)}\left.\frac{\partial\Phi}{\partial r}\right|_{r=R_+}. \tag{26}$$

This reduction follows from the large separation between the optical branches of the two components.[23] These simplified boundary conditions have been satisfactorily tested against microscopic lattice dynamical calculations in Ref. 23.

Uncoupled solution. Using Eq. (20), the matching boundary condition $\vec{u}(R) = 0$ immediately leads to the eigenvalue equation

$$J_{l+1/2}(\mu_m) = 0, \quad m = 1, 2, \ldots \tag{27}$$

with the dispersion relation

$$\omega^2 = \omega_{\rm TO}^2 - \beta_T^2 \left(\frac{\mu_m}{R}\right)^2 . \tag{28}$$

The mechanical displacement is given by

$$\vec{u} = -iD_1\sqrt{l(l+1)}\frac{R}{\mu_m} j_l\left(\frac{\mu_m r}{R}\right)\vec{X}_{lm}(\theta,\varphi). \tag{29}$$

These solutions correspond to modes vibrating along $\vec{X}_{lm}$, completely decoupled from the other curvilinear components (along $\vec{e}_r$ and $\vec{e}_r \times \vec{X}_{lm}$ directions) and bearing what one may call a purely "transverse" character (with respect to the sphere radius and as exemplified by the curvature β_T^2 of the bulk TO branches). Equations (14), (17), and (18) indicate that these modes have no electrostatic potential associated with them. If the condition (27) is not fulfilled, then $D_1 = 0$ and the $\vec{X}_{lm}$ vibrational components are absent.

Coupled modes. The boundary conditions applied to the other two components of $\vec{u}$ give a homogeneous system of linear equations for the constants A_1, B_1, C_1, and C_2. For these states the following secular equation is found:

$$\nu_n j_l'(\nu_n) F_l(\mu_n) = l(l+1) j_l(\nu_n) G_l(\mu_n) , \tag{30}$$

where

$$F_l(\mu) = \frac{\omega_{\rm LO}^2 - \omega_{\rm TO}^2}{\beta_T^2}\left(\frac{R}{\mu}\right)^2 l\left[\mu g_l'(\mu) - l g_l(\mu)\right] + \left(l + \frac{\varepsilon_\infty^{(2)}}{\varepsilon_\infty^{(1)}}(l+1)\right)\left[\mu g_l'(\mu) + g_l(\mu)\right] , \tag{31}$$

$$G_l(\mu) = \frac{\omega_{\rm LO}^2 - \omega_{\rm TO}^2}{\beta_T^2}\left(\frac{R}{\mu}\right)^2 \frac{\varepsilon_\infty^{(2)}}{\varepsilon_\infty^{(1)}}\left[l g_l(\mu) - \mu g_l'(\mu)\right] + \left(l + \frac{\varepsilon_\infty^{(2)}}{\varepsilon_\infty^{(1)}}(l+1)\right) g_l(\mu) , \tag{32}$$

$$\mu = QR, \quad \nu = qR,$$

$$\left(\frac{\beta_L}{\beta_T}\right)^2 \nu^2 - \mu^2 = \frac{R^2}{\beta_T^2}(\omega_{\rm LO}^2 - \omega_{\rm TO}^2). \tag{33}$$

For the definition of g_l see Eq. (A7). In this case, $D_1 = 0$ and the vector $\vec{u}$ have two components

$$\vec{u} = u_r(r) Y_{lm}(\theta,\varphi)\vec{e}_r + u_3(\vec{r})\vec{e}_r \times \vec{X}_{lm}(\theta,\varphi) \tag{34}$$

with

$$u_r = A\left[-\frac{d}{dr}\left[j_l\left(\nu_n\frac{r}{R}\right)\right] + \frac{l(l+1)}{r} p_l g_l\left(\mu_n\frac{r}{R}\right) - \frac{t_l}{R} l\left(\frac{r}{R}\right)^{l-1}\right] , \tag{35}$$

$$u_3 = -iA\frac{\sqrt{l(l+1)}}{r}\left\{-j_l\left(\nu\frac{r}{R}\right) + p_l\frac{d}{dr}\left[r g_l\left(\mu\frac{r}{R}\right)\right] - t_l\left(\frac{r}{R}\right)^l\right\} , \tag{36}$$

$$p_l = \left\{\nu j_l'(\nu)\left[(\gamma+1)l + (l+1)\varepsilon_\infty^{(2)}/\varepsilon_\infty^{(1)}\right] + \gamma l(l+1) \times \left(\varepsilon_\infty^{(2)}/\varepsilon_\infty^{(1)}\right) j_l(\nu)\right\} / \{\, l(l+1)\,[\, l + (l + 1\left(\varepsilon_\infty^{(2)}/\varepsilon_\infty^{(1)}\right) g_l(\mu)\,]\,\} . \tag{37}$$

$$t_l = \gamma\left[\nu j_l'(\nu) + (l+1)\left(\varepsilon_\infty^{(2)}/\varepsilon_\infty^{(1)}\right) j_l(\nu)\right] / [\, l + (l+1)\varepsilon_\infty^{(2)}/\varepsilon_\infty^{(1)}\,] , \tag{38}$$

$$\gamma = \frac{\omega_{\rm LO}^2 - \omega_{\rm TO}^2}{\beta_T^2}\left(\frac{R}{\mu}\right)^2 . \tag{39}$$

In Eqs. (35) and (36) A is a normalization constant. It can be proved[24] that the eigensolutions (29) and (34) of the differential equations (1) and (3) obey the following orthogonality condition

$$\int \vec{u}_n^* \cdot \vec{u}_m \rho(r) dv = 0 \ \text{ if } \ n \neq m, \tag{40}$$

where the subindices n, m describe the different eigenvectors obtained from the dispersion relations (27) or (30). The set of functions $\{\vec{u}_n\}$ can be normalized such that[24]

$$\int \vec{u}_n^*(\vec{r}) \cdot \vec{u}_m(\vec{r}) \rho(r) dv = \delta_{n,m} . \tag{41}$$

The potential Φ obtained from Eqs. (14), (17), and (18) leads directly to a Fröhlich-type electron-phonon interaction. Following the procedure presented in Ref. 24, the electron-phonon Hamiltonian can be written as

$$H_{\rm int} = \sum_n \sum_{l=0}^{\infty} \sum_{m=-l}^{l} C_F \frac{R}{\nu_n}(2l+1) i^l \sqrt{2\pi} \times \bar{\Phi}_{\nu_n,l}(r) \cdot Y_{lm}(\theta,\varphi)(\hat{b}_{\nu_n} + \hat{b}_{-\nu_n}^\dagger), \tag{42}$$

with

$$\bar{\Phi}_{\nu_n,l}(r) = \begin{cases} \left[\nu_n j_l'(\nu_n) + (l+1)(\varepsilon_\infty^{(2)}/\varepsilon_\infty^{(1)}) j_l(\nu_n)\right]\left(\frac{r}{R}\right)^l \\ \quad - \left[l + (l+1)\varepsilon_\infty^{(2)}/\varepsilon_\infty^{(1)}\right] j_l\left(\nu_n\frac{r}{R}\right) , \\ r \leq R \\ \left[\nu_n j_l'(\nu_n) - l j_l(\nu_n)\right]\left(\frac{R}{r}\right)^{l+1} , \\ r \geq R, \end{cases} \tag{43}$$

and

$$C_F = e\sqrt{\frac{2\pi\hbar\omega_{\rm LO}}{V_0}(\varepsilon_\infty^{-1} - \varepsilon_0^{-1})}\ , \tag{44}$$

where $\hat{b}_\nu$ and $\hat{b}_\nu^\dagger$ are annihilation and creation operators for vibrational modes in the state ν and V_0 the crystal volume. By resonant Raman scattering the spherical ($l = 0$) and spheroidal quadrupolar modes ($l = 2$) can, in principle, be observed.[25] The spherical modes are excited for parallel polarizations of the incident and scattered light. The most important contribution to one-phonon Raman scattering corresponds to $l = 0$. In this case the $\vec{X}_{00}$ component is absent, thus, radial modes are only obtained. The corresponding eigenvalue equation can be obtained by setting the mechanical dispacement equal to zero:

$$\vec{u}_{l=0} = Aj_1\left(\nu_n \frac{r}{R}\right)\vec{e}_r\ . \tag{45}$$

Using well known properties of spherical Bessel functions this equation can be written as:

$$\tan\nu_n = \nu, \quad n = 1, 2, \ldots\ . \tag{46}$$

The corresponding vibrational frequencies are of the longitudinal type, given by [see Eq. (12)]:

$$\omega^2 = \omega_{\rm LO}^2 - \beta_L^2\left(\frac{\nu_n}{R}\right)^2\ . \tag{47}$$

The Fröhlich electron-phonon interaction Hamiltonian is

$$H_{\rm int}^{l=0} = \sum_n C_F \frac{R}{\nu_n}\frac{\varepsilon_\infty^{(2)}}{\varepsilon_\infty^{(1)}}\left[j_0(\nu_n) - j_0\left(\nu_n\frac{r}{R}\right)\right] \times(b\gamma_n + \hat{b} - \gamma_n)\ . \tag{48}$$

Figure 1 shows the phonon energies of the first three modes of a GaAs dot in AlAs for $l = 0$ as a function of the quantum dot radius. Note that the $n = 1$ mode occurs basically at the $\omega_{\rm LO}$ frequency of the dot material, except for radii $R \lesssim 25$ Å. The modes of higher n begin to decrease in frequency at larger radii.

The frequencies of the coupled modes are more difficult to obtain since they require the solution of the rather complicated Eq. (30). In the limiting case of R large [this means μ and ν large but R smaller than the wavelength of light corresponding to the $(\omega_{\rm TO}, \omega_{\rm LO})$ frequency range] it is easy to see that Eq. (30) reduces to

$$J_l'(qR)g_l'(QR)\left[\frac{\omega_{\rm LO}^2 - \omega_0^2}{\beta_T^2}\frac{l}{Q} + Q\left(l + \frac{\varepsilon_\infty^{(2)}}{\varepsilon_\infty^{(1)}}(l+1)\right)\right] = 0 \quad \text{for} \quad R \to \infty. \tag{49}$$

From the above equation and (10) it follows that

$$\omega^2 = \omega_{\rm TO}^2\frac{\varepsilon_0 l + \varepsilon_\infty^{(2)}(l+1)}{[\varepsilon_\infty^{(1)} l + \varepsilon_\infty^{(2)}(l+1)]}. \tag{50}$$

According to Eq. (50) a series of modes with frequencies between $\omega_{\rm TO}$ and $\omega_{\rm LO}$ is obtained (for a review see Ref. 3). For $l = 1$ the so-called Fröhlich frequency[1] $\omega_F^2 = \omega_{\rm TO}^2(\varepsilon_0^{(2)} + 2\varepsilon_\infty^{(2)})/(\varepsilon_\infty^{(1)} + 2\varepsilon_\infty^{(2)})$ is derived. The three degenerate Fröhlich modes correspond to a uniform polarization of the sphere. The modes with $l > 1$ are usually called *surface modes*. Note that the modes of Eq. (50), obtained in the limit $R \to \infty$ are not affected by the mechanical boundary conditions: they are basically the same as obtained by imposing only electrostatic boundary conditions on Φ. If R is not much larger than Q^{-1} and q^{-1} the effect of the mechanical boundary conditions becomes important and Eq. (50) is no longer valid.

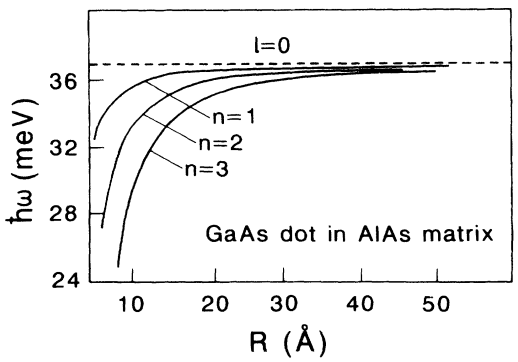

FIG. 1. The optical vibrational energies of the first three $l = 0$ modes in a spherical QD as a function of R. The parameters of Ref. 23 for GaAs imbedded in AlAs have been used in the calculation.

IV. DISCUSSION

In Sec. III we have obtained two kinds of modes, one of them is relatively simple, its displacement $\vec{u}$ being given in Eq. (29) in terms of $\vec{X}_{lm}(\theta,\varphi)$ [defined in Eq. (A11)]. It is easy to see that the *vector* $\vec{U} = \vec{X}_{lm}(\theta,\varphi)$ has, upon inversion with respect to the center of the sphere, a parity opposite to that of $Y_{lm}(\theta,\varphi)$: it is even for $l = 1, 3$ and odd for $l = 2, 4$. These "uncoupled" modes correspond to the torsional modes of Ref. 25 where, however, only elastic vibrations of a sphere with a zero stress boundary condition were considered. Although the case under consideration here, i.e., optical modes of a GaAs sphere imbedded in AlAs, is rather different, the symmetry considerations are similar: the solutions of Eq. (1) must belong to the irreducible representations of the three-dimensional rotation-inversion group $O(3)$ labeled as D_l^g and D_l^u (g and u mean even or odd upon inversion). The uncoupled modes belong to D_1^g, D_2^u, D_3^g while the mixed (spheroidal) modes belong to $D_0^g, D_1^u, D_2^g, \ldots$.

The dipole operator responsible for ir absorption belongs to D_1^u while the Raman transition operator for dipole-allowed scattering (a second rank tensor) belongs to D_0^g and D_2^g. Hence the torsional modes are not expected to be optically active.

The discussion above is valid for the solutions of Eqs. (1) and (3) which are only an approximation to the

macroscopic vibrations of a zinc-blende-type material. Even within the quadratic expansion of the bulk dispersion relations versus wavevector, Eq. (1) does not reflect the cubic, T_d symmetry of a material like GaAs or even silicon (O_h) [some of the data in the literature[16] have been obtained for hexagonal, wurtzite-type materials such as CdS and CdSe. A generalization of Eq. (1) to cover this case is also possible]. The first noticeable problem in the case of T_d symmetry is the lack of inversion symmetry. Furthermore among the operations of $O(3)$, only those which bring a tetrahedron onto itself are symmetry operations of T_d: the sphere has preferred axes which correspond to the crystal axes of the base material. The lack of inversion symmetry corresponds to the fact that the [111] direction is not equivalent to $[\bar{1}\bar{1}\bar{1}]$, represented in our treatment by the finite value of α and its sign introduced in Eqs. (2) and (3). Note that a reversal of the sign of α produces, according to Eq. (3), a reversal of the sign of Φ.

In the case of a silicon sphere imbedded, e.g., in germanium, $\alpha = 0$ and no electrostatic effects occur nor are there dipole-allowed ir modes (in the spirit of the microscopic model we neglect, of course, symmetry breaking at the interface which may induce ir activity: note that the Ge-Si bond is ir active).[26] The D_0^g modes correspond to the Γ_1^+ O_h symmetry and are Raman active, the scattering being fully *polarized* independently of scattering configuration. A calculation of the Raman cross section for these modes would be rather interesting but is beyond the scope of this paper. A microscopic calculation based on the electronic band structure and a supercell with the sphere at its center[27] would, in principle, be possible but rather formidable. One based on bond polarizability models would probably suffice to unravel the main features of the phenomenon. It is clear that the $l = 0$, $n = 1$ mode should have the strongest cross section. Like in the case of planar superlattices, higher n modes should be weaker because of the scattering amplitude cancellations which result from their oscillatory nature.

We should emphasize the fact that the fully polarized scattering of the D_0^g (Γ_1^+) modes has no counterpart in bulk crystals which exhibit $\Gamma_{25'}$ (diamond) or Γ_{15} (zinc blende) symmetry scattering with a depolarization ratio of 0.75. The question, thus, immediately arises of when, upon increasing R, the sphere will behave as a piece of bulk material. The treatment given here implies *coherence* of the vibrational mode throughout the whole sphere and, for zinc blende materials, over some region outside of the sphere. Hence, the qualitative answer to the question just posed is that the radius R must be smaller than the vibrational coherence length ξ, a quantity which can be estimated from the phonon lifetime τ and their group velocity $v_g = \beta^2 q/\omega$,

$$\xi = \frac{\beta^2 q}{\omega} \cdot \tau \simeq \frac{\pi \beta^2}{\omega R} \tau \,. \tag{51}$$

Typical bulk values of $\tau = 10^{-11}$ sec and $\beta = 3.5 \times 10^5$ cm sec^{-1} yield $\xi = 200$ Å for $R = 25$ Å. Hence for such small spheres the $l = 0$, $n = 1$ mode should be coherent. Figure 1 indicates that the frequency of this mode should lie only 0.4 meV (3 cm^{-1}) below the bulk LO frequency. If the vibration is coherent throughout the whole sphere one can also ask what happens to the Γ_1 Raman activity as the sphere radius becomes larger (while keeping coherence). This question becomes more acute when one considers that a Ge tetrahedron imbedded in Si has Γ_1 Raman activity, while bulk germanium does not. It is clear that the Γ_1 Raman activity of a Ge sphere must arise from the changes in surface bonds cut by the sphere boundary (Ge-Si bonds), which are different from the Ge-Ge bonds inside the sphere. Hence, the Γ_1 activity must be, in this case, a surface effect. It should depend on the exact nature of the spherical interface, e.g., on whether an atom or a midband is at the center of the sphere.

The corresponding Γ_1 modes of a GaAs sphere are LO-like [Eq. (47)] and the Raman scattering amplitude should have a component produced by the Fröhlich interaction represented by Eq. (48) since the corresponding charges (i.e., C_F's) are opposite for electrons and holes.[15] A net effect results only from the fact that the confined electron and hole states of the GaAs dot penetrate differently into the AlAs barrier because of the different effective masses. This may explain the observation of bulk LO frequencies in small polar semiconductor particles imbedded in glass, which until now has not been understood.[16]

Let us consider the Raman active D_2^g modes. Upon lowering the symmetry to the O_h of silicon T_d of GaAs the D_2^g representation of $O(3)$ becomes $\Gamma_{25'}^+$ (Γ_{15}). These symmetries are also Raman active in the bulk and, as mentioned above, lead to partly depolarized scattering. A closer investigation of the frequencies and cross sections of these modes is beyond the scope of this work. We should mention, however, that the ir-active D_1^u dipole and surface modes also convert into Γ_{15} in zinc blende and are thus Raman active. The corresponding electron-phonon interaction can occur either through the electrostatic potential Φ [Fröhlich Hamiltonian of Eq. (42)] or directly through $\vec{u}$ (deformation potential interaction). The polarization selection rules should be the same as those of the bulk: they could be investigated by studying the scattering of a coherently oriented array of quantum dots. These modes should also be strongest for $n = 1$. In the case of randomly oriented spheres, such as those fabricated in glass matrices, one should be able to observe the average depolarization ratio of 0.75.

In the limit of large radius the $l = 1$ modes should occur at the Fröhlich frequency [Eq. (50) for $l = 1$]:

$$\omega_F^2 = \frac{\omega_{\mathrm{LO}}^2 + 2\omega_{\mathrm{TO}}^2}{3}, \tag{52}$$

where we have made the assumption $\varepsilon_\infty^{(2)} \simeq \varepsilon_\infty^{(1)}$, valid in the case of GaAs imbedded in AlAs.

The Fröhlich frequency is usually seen in ir absorption[3,28] but not in Raman scattering.[16]

V. CONCLUSION

We have developed a systematic treatment of the long-wavelength polar optical phonons and the electrostatic

electron-phonon interaction in quantum dots. Our treatment involves a complete formulation of the matching problem and of the mechanical and electrostatical fields. Explicit solutions of the 4×4 system of differential equations for spherical quantum dots have been studied and analytical expression for the Fröhlich type electron-phonon interaction derived. We have shown that the model gives (i) transverse uncoupled modes ($\vec{X}_{lm}$ component) below the bulk TO frequency ω_{TO}, and (ii) modes with mixed LO-TO character involving two components of the vibrational amplitudes ($\vec{e}_r$ and $\vec{e}_r \times \vec{X}_{lm}$ components) and the electrostatical potential. The $l = 0$ modes have been investigated in detail for any value of the radius R and also the mixed modes with $l \neq 0$ in the limit of large R. The dielectric model for surface phonons has been rederived as a particular case ($R \to \infty$) of the general dispersion relation given in Eq. (30). A qualitative discussion of the implications of our work for Raman and ir spectroscopy of spherical quantum dots has been given.

ACKNOWLEDGMENTS

One of us (C.T.-G.) acknowledges the hospitality of the Max-Planck-Institut für Festkörperforschung where part of this work was performed. We thank M.P. Chamberlain for a critical reading of the manuscript.

APPENDIX

We consider here the solutions of the vectorial Eq. (9) and introduce the most convenient basis for the treatment of a spherical quantum dot. The vectorial character of Eq. (9) leads to two kinds of difficulties: first, the structure of $\vec{\nabla}^2\vec{\Gamma}$ is very complicated in curvilinear coordinates; second, owing to the fact that $\vec{\Gamma} = \vec{\nabla} \times \vec{u}$, the components of $\vec{\Gamma}$ are not independent but are related by the equation

$$\vec{\nabla} \cdot \vec{\Gamma} = 0. \tag{A1}$$

Hence, if $\{e_i\}$ $(i = 1, 2, 3)$ is a curvilinear basis, only two components of $\vec{\Gamma}$ are independent, because of Eq. (A1). Thus, it is enough to obtain general solutions for two of these components $\Gamma_i\vec{e}_i$ of $\vec{\Gamma}$. $\Gamma_i\vec{e}_i$ should be a solution of Eq. (9) and, due to (A1), $\Gamma_i\vec{e}_i$ must be the rotational of certain vector field. It can be shown that we may choose[29]

$$\vec{M} = \vec{\nabla} \times (v_1\vec{r}) \tag{A2}$$

and

$$\vec{N} = \frac{1}{Q}\vec{\nabla} \times \vec{\nabla} \times (v_2\vec{r}) \tag{A3}$$

as independent solutions of Eq. (9) and Eq. (A1), where v_1 and v_2 are solutions of the scalar Helmholtz equation[29]

$$(\vec{\nabla}^2 + Q^2)v_i = 0 \quad (i = 1, 2). \tag{A4}$$

Hence, the vector $\vec{\Gamma}$ is equal to

$$\vec{\Gamma} = \vec{M} + \vec{N}\ . \tag{A5}$$

In a quantum dot ($r < R$), the solutions of (A4) which are bounded for $r \to 0$ can be written as

$$v \sim g_l(Qr)Y_{lm}(\theta, \varphi), \tag{A6}$$

$$g_l(Qr) = \begin{cases} j_l(Qr), & Q^2 > 0 \\ i_l(Qr), & Q^2 < 0\ , \end{cases} \tag{A7}$$

where i_l is the modified spherical Bessel function. For further calculations the following vectorial identities

$$\vec{M} = (\vec{\nabla}v_1) \times \vec{r}\ , \quad \vec{\nabla} \times \vec{N} = Q(\vec{\nabla}v_2) \times \vec{r}, \tag{A8}$$

$$\vec{\nabla} \times \vec{\nabla} \times \vec{N} = \vec{\nabla}\vec{\nabla} \cdot \vec{N} + Q^2\vec{N} \tag{A9}$$

are needed. It is convenient to write the operator $\vec{\nabla}$ as[30]

$$\vec{\nabla} = \vec{e}_r\frac{\partial}{\partial r} - \frac{i}{r}\vec{e}_r \times \vec{L}, \tag{A10}$$

$\vec{L}$ being an operator given by $\vec{L} = -i\vec{r} \times \vec{\nabla}$ and $\vec{e}_r$ a unitary vector along the $\vec{r}$ direction. We have used the notation

$$\vec{X}_{lm} = \frac{\vec{L}Y_{lm}}{\sqrt{l(l+1)}}, \quad l \neq 0. \tag{A11}$$

In spherical basis $\vec{X}_{lm}$ is given by

$$\vec{X}_{lm}(\theta, \varphi) = \frac{\sqrt{l(l+1)}}{(2l+1)\sin\theta}\left[m\frac{(2l+1)}{l(l+1)}iY_l^m\vec{e}_\theta - \left(\frac{l-m+1}{l+1}Y_{l+1}^m - \frac{l+m}{l}Y_{l-1}^m\right)\vec{e}_\varphi\right]. \tag{A12}$$

For $l = 0$, because Y_{00} is a constant, we define $\vec{X}_{00} = 0$. For calculating $\vec{u}$ it is necessary to obtain $\vec{M}$ and $\vec{\nabla} \times \vec{N}$. These vectors can be found from Eq. (A8) making use of Eq. (A10):

$$\vec{M} = -iB_1\sqrt{l(l+1)}g_l\vec{X}_{lm}, \qquad \vec{\nabla} \times \vec{N} = -iQD_1\sqrt{l(l+1)}g_l\vec{X}_{lm}. \tag{A13}$$

The evaluation of $\vec{\nabla} \times \vec{M}$ can be simply performed using (A10) in (A13) while the vector $\vec{N}$ is derived using the vectorial identity (A9). The final expressions for $\vec{\Gamma}$ and $\vec{\nabla} \times \vec{\Gamma}$ are

$$\vec{\Gamma} = -iB_1\sqrt{l(l+1)}g_l\vec{X}_{lm} - iD_1\frac{\sqrt{l(l+1)}}{Qr}\left[i\sqrt{l(l+1)}g_lY_{lm}\vec{e}_r + \frac{d}{dr}(rg_l)\vec{e}_r \times \vec{X}_{lm}\right] \tag{A14}$$

and

$$\vec{\nabla}\times\vec{\Gamma}=-iB_1\frac{\sqrt{l(l+1)}}{r}\left[\,i\sqrt{l(l+1)}g_l Y_{lm}\vec{e}_r + \frac{d}{dr}(rg_l)\vec{e}_r\times\vec{X}_{lm}\,\right]-iQD_1\sqrt{l(l+1)}g_l\vec{X}_{lm}\,. \tag{A15}$$

Hence, the curvilinear basis $(\vec{e}_r,\ \vec{X}_{lm},\ \vec{e}_r\times\vec{X}_{lm})$ appears naturally. Substituting Eqs. (17), (18), and (A15) in Eq. (16) the mechanical displacement vector for the optical modes of a spherical quantum dot [Eq. (20)] is obtained.

* Also at Department of Theoretical Physics, Havana University, Vedado, 10400 Havana, Cuba.

[1] H. Fröhlich, *Theory of Dielectrics* (Oxford University Press, Oxford, 1948).

[2] R. Fuchs and K.L. Kliewer, Phys. Rev. **140**, A2076 (1970).

[3] R. Ruppin and R. Englman, Rep. Prog. Phys. **33**, 149 (1970).

[4] C. Trallero-Giner, F. Garcia-Moliner, V.R. Velasco, and M. Cardona, Phys. Rev. B **45**, 11 944 (1992).

[5] E. Duval, A. Boukenter, and B. Champagnon, Phys. Rev. Lett. **56**, 2052 (1986).

[6] A.I. Ekimov, Phys. Scr. **T39**, 217 (1991).

[7] W. Hansen, T.P. Smith III, K.Y. Lee, J.A. Brum, C.M. Knoedler, J.M. Hong, and D.P. Kern, Phys. Rev. Lett. **62**, 2168 (1989).

[8] Ch. Sikorski and U. Merkt, Phys. Rev. Lett. **62**, 2164 (1989).

[9] J. Alsmeier, E. Batke, and J.P. Kotthaus, Phys. Rev. B **41**, 1699 (1990).

[10] M. Fujii, S. Hayashi, and K. Yamamoto, Appl. Phys. Lett. **57**, 2692 (1990).

[11] A. Tanaka, S. Onari, and T. Arai, Phys. Rev. B **45**, 6587 (1992).

[12] S. Hayashi and R. Ruppin, J. Phys. C **18**, 2583 (1985).

[13] S. Hayashi and H. Kanamori, Phys. Rev. B **26**, 7079 (1982).

[14] A. Tanaka, S. Onari, and T. Arai, Phys. Rev. B **47**, 1237 (1993).

[15] See, for instance, B. Jusserand and M. Cardona, in *Light Scattering in Solids V*, edited by M. Cardona and G. Güntherodt (Springer, Heidelberg, 1989), p. 139.

[16] M.C. Klein, F. Hache, D. Richard, and C. Flytzanis, Phys. Rev. B **42**, 11 123 (1990).

[17] S. Nomura and T. Kobayashi, Phys. Rev. B **45**, 1305 (1992).

[18] B.K. Ridley, Phys. Rev. B **44**, 9002 (1991).

[19] L. Landau and E.M. Lifshitz, *Course of Theoretical Physics*, Theory of Elasticity, Vol. 7 (Pergamon, Oxford, 1970).

[20] F. Comas and C. Trallero-Giner, Physica B (to be published).

[21] F. Comas, C. Trallero-Giner, and A. Cantarero, Phys. Rev. B **47**, 7602 (1993).

[22] M. Born and K. Huang, *Dynamical Theory of Crystal Lattices* (Clarendon, Oxford, 1988).

[23] F. Comas, R. Pérez-Alvarez, C. Trallero-Giner, and M. Cardona, Superlatt. Microstruct. (to be published); M.P. Chamberlain, M. Cardona, and B. Ridley, Phys. Rev. B **48**, 14 356 (1993).

[25] E. Duval, Phys. Rev. B **46**, 5795 (1992).

[26] U. Schmid, N.E. Christensen, and M. Cardona, Phys. Rev. B **41**, 5919 (1990).

[27] C.H. Grein and M. Cardona, Phys. Rev. B **45**, 8328 (1992).

[28] T.P. Martin, Phys. Rev. B **1**, 3480 (1970); L. Genzel and T.P. Martin, Phys. Status Solidi B **51**, 91 (1972).

[29] P.M. Morse and H. Feshbach, *Methods of Theoretical Physics* (McGraw Hill, New York, 1953).

[30] J.D. Jackson, *Classical Electrodynamics*, 2nd ed. (Wiley, New York, 1975), p. 767.